

Minimum vehicle slip path planning for automated driving using a direct element method

Kanarachos, S. , Blundell, M.V. and Kanarachos, A.

Author post-print (accepted) deposited in CURVE September 2015

Original citation & hyperlink:

Kanarachos, S. , Blundell, M.V. and Kanarachos, A. (2015) Minimum vehicle slip path planning for automated driving using a direct element method. Proceedings of the Institution of Mechanical Engineers, Part D: Journal of Automobile Engineering, volume (in press).

<http://pid.sagepub.com/> 

Note: Article in press, full citation details will be updated once available.

Copyright © and Moral Rights are retained by the author(s) and/ or other copyright owners. A copy can be downloaded for personal non-commercial research or study, without prior permission or charge. This item cannot be reproduced or quoted extensively from without first obtaining permission in writing from the copyright holder(s). The content must not be changed in any way or sold commercially in any format or medium without the formal permission of the copyright holders.

This document is the author's post-print version, incorporating any revisions agreed during the peer-review process. Some differences between the published version and this version may remain and you are advised to consult the published version if you wish to cite from it.

CURVE is the Institutional Repository for Coventry University

<http://curve.coventry.ac.uk/open>

Title:

Minimum vehicle slip path planning for automated driving using a direct element method

Stratis Kanarachos*, Mike Blundell* and Andreas Kanarachos⁺

*Faculty of Engineering & Computing, Coventry
University
3, Gulson Road, Coventry, U.K.
CV1 2JH

⁺Mechanical Engineering Department, Frederick
University
7, Y. Frederickou Str., Nicosia, Cyprus
1036

Corresponding author: Stratis Kanarachos,
Faculty of Engineering and Computing,
Coventry University, 3, Gulson Road, Coventry
CV1 2JH, stratis.kanarachos@coventry.ac.uk

Abstract

In the UK the number of fatal accidents on rural roads is approximately double the one on urban. Statistics also showed that rural accidents decreased less than on other road types. The narrow width and complex geometry are less forgiving to drivers' mistakes. A potential remedy for this problem is automated driving (AD). Decisive in AD is the ability to plan safe and feasible paths that can match any road geometry. Different methods have been proposed for this purpose. Most of them either utilise forward simulation of a vehicle dynamics model or describe mathematically a reference path and then track it. In this paper, a new method belonging to the latter category is presented. The method is based on a direct element approach and, as will be shown and discussed, is unique because it's the first one that includes a prediction of the vehicle slip angle and designs paths minimising their maximum value. Furthermore, it is very flexible because it can plan paths under arbitrary boundary and intermediate conditions and has a low computational burden. Simulations illustrate its performance and comparisons to other known methods highlight its strengths.

Keywords: path planning, automated driving, minimum slip angle, direct element method

Date received 10 August 2015

J. Automobile Engineering

List of notations

Symbol	Variable
a	acceleration
α	Tire slip angle
b	Element coefficient
c	Element coefficient
d	Element coefficient
F	Tire force
g	Gravitational acceleration
i	Iteration number
l	Vehicle width
l_f	Distance from front axle to center of gravity
l_r	Distance from rear axle to center of gravity
m	Mass
n	Number of element
N	Total number of elements
u_f	Longitudinal velocity
v	Lateral velocity
r	Yaw rate
$t_{n\ span}$	Element time span
$t_{n\ span}^{i+1,cmd}$	Commanded element time span
A_n	Element matrix
C	Cornering stiffness

I_z	Mass moment of inertia
M	Moment
δ	Steering input
δF	Load transfer
κ	User defined coefficient
μ	Tire-road friction coefficient

Subscript

Meaning

a	First element node
b	Second element node
c	Constraints
f	Front tire
max	Maximum value
n	Element number
r	Rear tire
u	Unknowns
y	Lateral direction
z	Vertical direction
I, II, \dots	Increasing number
$1, 2, \dots$	Increasing number

Superscript

Meaning

i	Iteration number
-----	------------------

1. Introduction

In the last decade progress towards improving road safety has been achieved through advancements in vehicle's passive and active safety [1] - [4]. No doubt, most of the car accidents happen because of human mistakes in decision making and handling of the vehicle. Various Advanced Driver Assistance Systems (ADAS) have been and are being developed to reduce drivers' mistakes. According to the German In-Depth Accident Study (GIDAS) lateral collision avoidance systems have the potential to reduce by up to 24% the total number of rear end car accidents [5]. Vehicle manufacturers and suppliers envision reducing fatalities and serious injuries to zero [6].

In the UK the number of fatal accidents on rural roads is approximately double the one on urban [7]. Statistics also showed that accidents decreased less than on other road types. The narrow width and complex geometry are less forgiving to drivers' mistakes. A potential remedy for this problem is automated driving (AD). Decisive in AD is the ability to plan safe and feasible paths that can match any road geometry. For this purpose, different methods have been proposed up to now. The methods can be broadly classified in two categories.

In the first category a vehicle model is utilised for determining the best reference path. The solution is calculated by iteratively performing forward simulations in order to optimise an objective. Numerous variants of this approach exist.

One variant are the sampling based algorithms, frequently used in robotics [8]-[10]. The most well known sampling based algorithm is the Rapid-exploring Random Tree (RRT) and its extensions. Sampling-based algorithms are applicable to very general dynamical models and they do not require the explicit enumeration of constraints, but

allow trajectory-wise checking of possibly very complex constraints. The algorithm solves for the input to the vehicle $u(t)$ either by randomly sampling an input itself or by sampling a configuration and reverse calculating $u(t)$, typically with a lookup table. The feasibility of the output is checked against vehicle and environmental constraints, such as rollover and obstacle avoidance constraints. Sampling based algorithms have been employed mostly on vehicles at very low speeds and for smooth trajectories [11]. For this reason, in many papers, simple vehicle models -e.g. a Dubins car or a point mass which do not consider vehicle side slip- are employed. The computational burden of sampling based algorithms is an issue since they require the iterative solution of a differential equation. Furthermore, complex space constraints can significantly decrease their performance.

Another variant is Model Predictive Control (MPC) [12]-[14]. In some studies that employ MPC the vehicle navigation problem is formulated as an optimal control problem with constraints bounding a navigable region of the road surface [15]. In such a formulation, a constraint planner iteratively predicts, over a horizon, the safe corridor by use of sensor data and estimated behaviour of hazards and host vehicle [16]. The safe corridor is presented as lateral position constraint vector and is used, together with the vehicle dynamics prediction model, to compute an optimal sequence of control inputs and the associated vehicle trajectory while optimizing the vehicle performance characteristics. An optimal input sequence is computed, in each iteration, from which only the first step is implemented. The control input is obtained as the solution of a nonlinear programming (NLP) problem using a numerical optimisation algorithm [17]. In other studies instead of a corridor a fixed reference path is given e.g. the trace of a leading vehicle [18], [19]. In

those cases the objective is - under the operating constraints - to follow the reference path without hitting the obstacles. In MPC various vehicle dynamics models have been utilised. The most popular is the bicycle model with two degrees of freedom; yaw rate and lateral velocity. Recently bicycle vehicle models considering also the longitudinal and lateral load transfer during manoeuvring have been studied [20]. The computational burden is an issue also in MPC. In many cases simpler vehicle models have been utilised for reducing the computational cost [9], [21]. Another option is to reduce the prediction horizon. The disadvantage of a very short prediction horizon is that the vehicle becomes mainly reactive which may lead to significant performance degradation and stability problems.

A third variant of the first category is the optimal control framework [22], [23]. In this framework, the trajectories are computed as the solution to an optimization problem that seeks to minimize the manoeuvring time. Optimal control solutions for typical driving scenarios using tyre and chassis models of different complexities have been studied and the results were extensively analysed and discussed. One of the main conclusions was that the tyre model has a fundamental influence on the resulting control inputs [24]. One of the very interesting and important conclusions was that a few-state single-track vehicle model combined with different tire models is able to replicate the behaviour of experienced drivers [25]. The time optimal control optimization problem is challenging, since the time-optimality implies that the tire-friction models operate on the boundary of their validity. Furthermore, the numerical solution of a dynamic optimization problem where the time horizon is free is in general more demanding than solving a problem with fixed time horizon, because it adds additional degrees of freedom. In some cases it was

found that the optimization may not converge without proper initialization of the model trajectories prior to the optimization. Again the main drawback of this variant is the large computational cost. A potential solution is to store the optimal manoeuvres in a manoeuvre automaton. However, this inhibits significantly flexibility [26].

In the second category, the reference path is designed based on a mathematical path description. A number of assumptions is employed without the requirement to perform forward simulations of any vehicle model. The methods in this category are computationally fast. On the other hand it is possible to design paths which are incompatible to the vehicle's dynamics [27], [28] contrary to the methods belonging to the first category where a vehicle model and its dynamics (yaw, slip) are taken into account. This is a serious drawback and therefore a lot of methods focused on generating smooth paths [29], [30]. The main idea is that by controlling the path's dynamics it is possible to influence favourably a vehicle's path tracking performance.

In [31] the reference path was parameterized using two sixth order polynomials. The polynomials' unknown coefficients are computed by formulating the problem as a constrained minimum travelling distance problem and by respecting the desired conditions (position, velocity and acceleration) at the manoeuvre's boundaries. Main disadvantages of the method are that limits on acceleration and vehicle slip angle are ignored and that high order polynomials may present oscillatory behaviour. A further drawback is that the starting solution is a straight line. Thus, if there is not enough time to calculate an optimised solution the most probable outcome is a collision.

In reference [32] the authors employed a sigmoidal-7th degree polynomial to parameterize the reference path. The polynomial's coefficients are determined based on

the desired lateral jerk acceleration, velocity and position at the path's boundaries and by the allowable lateral acceleration. The manoeuvring time is calculated based on a shape factor which holds only for zero boundary conditions. Weaknesses of the method are that vehicle slip angle limitations are ignored and the lack of flexibility to define any intermediate path conditions.

The authors in [33] used a sigmoide to describe the reference path. The sigmoide is defined using three parameters which are chosen according to the driving situation such that the evasive path length is minimal. Limitations regarding the maximum lateral acceleration, maximal jerk and dynamics of the steering actuator are taken into account. In that regard a nonlinear constrained optimization problem has to be solved. The method has the drawback of neglecting vehicle slip angle limitations as well as the lack of flexibility to define intermediate path conditions. Furthermore, lateral velocity and acceleration have to be zero at the boundaries of the path.

However, in automated driving very complex scenarios may take place. To that respect the authors in [34] presented a methodology for designing reference paths under arbitrary boundary and intermediate conditions. The methodology, which is based on a direct element concept, makes possible to define not only the conditions at the boundaries of the path but also at any number of intermediate points. Furthermore, the boundary conditions can take any values, so it works for straight and curved road segments. Additionally, due to the fact that lower order blending functions are utilized it is possible to easily calculate the maximum position, angular velocity, acceleration and jerk values in each element and thus check whether any constraint is violated. Another advantage of

the method is that the starting solution is a collision free path. On the other hand vehicle slip angle limitations were neglected.

Surprisingly, up to now, most of the proposed “geometric” paths planning methods (second category) ignore the role of vehicle slip angle. However, it is well known that slip determines the vehicle’s manoeuvrability and that excessive slip angles may lead to instability. In this paper, the methodology presented in [34] is extended to include the vehicle slip angle. In a simple and computationally efficient way it is shown how to plan and predict the slip angle for a reference path and how to compute the respective steering input. Furthermore, a heuristic iterative algorithm that computes paths with minimized maximum slip angle is presented. Numerical simulations illustrate the performance of the method and show its strengths. For this purpose, the method is also compared to other known methods in the literature. Finally, a comparative analysis has been conducted to highlight the influence of vehicle properties on the optimized reference path.

The rest of the paper is organized as follows. In section 2 the vehicle model and direct element approach are discussed. In section 3 the slip angle prediction and heuristic optimisation algorithms are presented. In Section 4 the path planner is evaluated for a number of driving scenarios and compared to methods known from the literature. The simulations and analysis are performed in Matlab. In Section 5 a comparison is made between the optimized paths obtained for two different vehicle configurations. In Section 6 conclusions and future research directions are drawn.

2. Mathematical model

2.1 Consideration of vehicle slip angle in “geometric” path planning

In order to relate a vehicle’s slip angle to the dynamics of a reference path a vehicle model needs to be utilized. Since a very detailed vehicle dynamic model can be difficult to obtain and use, this paper uses a model that approximates vehicle motion with a reasonable accuracy for the application in mind [35], [36].

The two track vehicle model (TTVM), shown in Figure 1, is employed to derive the equations of motion described by lateral velocity v and yaw rate r [37]. The inherent limitations of the TTVM model apply to the proposed method. It will not approximate vehicle motion well at very low speeds, during tight manoeuvres or during high speed manoeuvring where the influence of suspension geometry is critical. It is also known from [10] that the linear bicycle model is valid only when $F_{y\max} < \frac{1}{3} \cdot \mu \cdot F_z$, effectively for lateral accelerations up to 0.4 g’s for dry road conditions and 0.05 g’s on icy conditions. However, it is highlighted that a well thought vehicle control strategy can compensate the vehicle nonlinearities, as shown in [35].

For simplification reasons the forward vehicle velocity u_f is assumed constant and therefore the longitudinal dynamics is neglected. The equations of motion, Eq. (1)-(2), are:

a)

b)

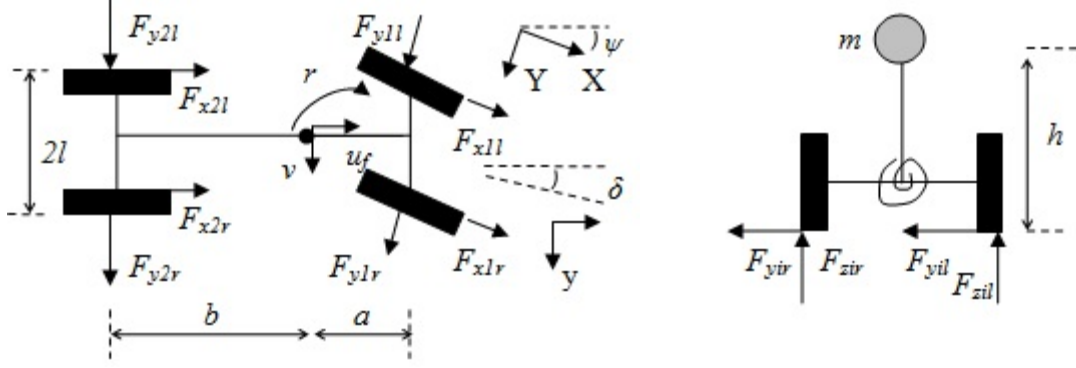


Figure 1. Top (a) and front (b) view of the vehicle model

$$m \cdot (\dot{v} + r \cdot u_f) = F_{yf} + F_{yr} \quad (1)$$

$$I_z \cdot \dot{r} = \sum M = l_f \cdot F_{yf} - l_r \cdot F_{yr} \quad (2)$$

where l_f , l_r are the distances from the front and rear axle to the centre of gravity respectively and F_{yf} , F_{yr} the lateral tire forces on the front and rear axle.

Tire forces (unless balanced) are expected to reduce velocity when slip angles are present. This is due to the fact that slip angles generate tire force components that oppose velocity. For small slip angles the influence is negligible but for high slip angles the effect is considerable. However, due to the fact that the vehicle slip angle β is bounded it is expected that their influence will be -in most cases- limited [38]. In any case, other parameters such as aerodynamic resistance and engine-gearbox friction losses will also cause a reduction in forward velocity u_f . A reduction in forward velocity u_f means that the vehicle will cover less distance both in longitudinal X and lateral direction Y . Thus, in order to avoid near miss cases the desired boundary conditions should be defined considering a reasonable safety factor.

Vehicle yaw rate r is limited either due to the finite tire-road friction μ or because of the bounded load transfer limit δF_z . In the first case, the yaw rate limit $r_{\max, I}$ is determined as follows:

$$a_y = \dot{v} + u_f \cdot r \leq a_{y\max} = \mu \cdot m \cdot g \Rightarrow \quad (3)$$

Since, $v = u_f \cdot \tan \beta$ we have that

$$a_y = u_f \cdot r + \dot{u}_f \tan \beta + \frac{u_f \cdot \dot{\beta}}{\sqrt{1 + \tan^2 \beta}} = u_f \cdot r + \frac{u_f \cdot \dot{\beta}}{\sqrt{1 + \tan^2 \beta}} \quad (4)$$

where β is the vehicle slip angle and therefore,

$$\left| r_{\max, I} \right| \leq \frac{1}{u_f} \cdot \left(\mu \cdot m \cdot g - \frac{u_f \cdot \dot{\beta}}{\sqrt{1 + \tan^2 \beta}} \right) \quad (5)$$

where g is the gravitational acceleration.

In the second case, for stability reasons, the load transfer δF_z during cornering is limited. By applying moment equilibrium in the roll direction we get:

$$\delta F_z = \frac{m \cdot a_y \cdot h}{2 \cdot l} \leq \delta F_{z_max} \quad (6)$$

where h is the height of centre of gravity and δF_{z_max} the allowable vertical load transfer. Combining Equations (4) and (6) gives the second bound $r_{max,II}$ of yaw rate:

$$|r_{max,II}| \leq \frac{1}{u_f} \cdot \left(\frac{2 \cdot \delta F_{z_max} \cdot l}{m \cdot h} - \frac{u_f \cdot \dot{\beta}}{\sqrt{1 + \tan^2 \beta}} \right) \quad (7)$$

In the European Union it is mandatory for all new vehicles to have an Electronic Stability Control System (ESC) [38]. It is therefore assumed that the vehicle in this study will have one, e.g. like the one described in [39]. An ESC system is activated if the yaw rate r or slip angle β exceed their threshold values [38]. Thus, the assumption is made that slip angle β is also limited by β_{max} :

$$|\beta| \leq \beta_{max} \quad (8)$$

In Figure 2 a vehicle's transient response for two different configurations is shown. Although both yaw rates r converge to the same value, slip angles β are quite different. Therefore, it is reasonable to conclude that if only yaw rate limits are considered then it is possible to design paths that will cause loss of manoeuvrability or stability to the vehicle.

a)

b)

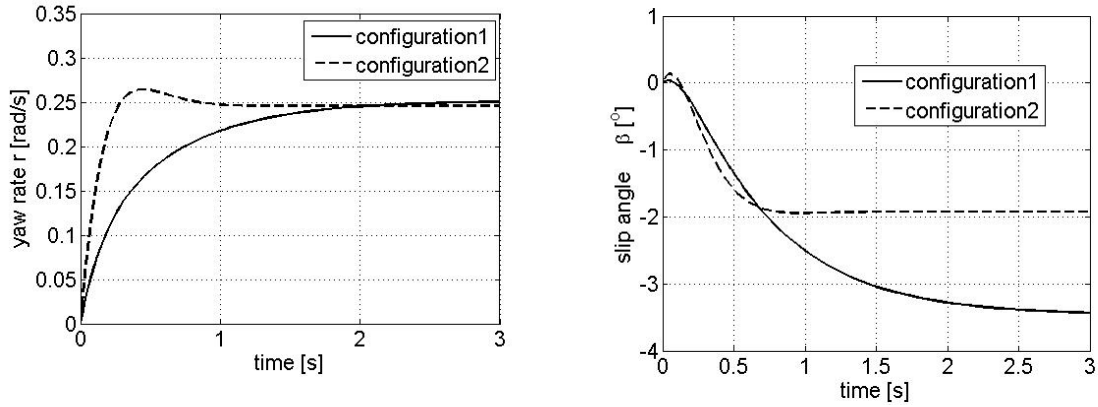


Figure 2. Yaw rate (a) and slip angle (b) transient response for two different vehicle configurations

2.2 *Direct element path planning method*

Although many methods already exist, path planning is still an active research topic as the recent body of literature shows. Advanced Driver Assistance Systems become more and more intelligent so that they can assist not only during critical events but also in “challenging” or near critical events too. Thus, they evolve from a “one shot” operation to a continuous one. The complexity of scenarios and the hard real time requirements to be met require algorithms that can handle flexibly very complex driving scenarios in minimum time. It is highlighted that a number of researchers formulate automated driving as a collision avoidance problem [21].

The direct element path planning method is a flexible and computationally efficient path planning method [34] because it can handle arbitrary boundary and intermediate path conditions and transforms a dynamic optimisation problem into an algebraic one. Since 2nd order and 3rd order blending functions are employed the maximum values of

yaw rate and slip angle in each element are calculated using simple algebraic formulas. Thus, it is computationally efficient to check whether any constraints were violated. Furthermore, it can work both in structured and unstructured environments where no clear road markings are available. Last but not least, as it will be shown, it performs much better than other “geometric” path planning methods.

The direct element method is briefly described in the following. A schematic of the approach is shown in Figure 3. The total path is decomposed in N elements/segments. Each element is denoted with a number $n=1\dots N$ and has two nodes: the start node n_a and end node n_b . The reference path is generated by joining the end node n_b and start node $(n+1)_a$ of two consecutive elements n and $n+1$, $n=1\dots N-1$. Each element is parameterized using two variables: time span $t_{n\text{span}}$ and the highest order constrained state variable, in this case the second derivative of yaw rate $\ddot{r}_n = d_{3n}$, $t_n \in [0, t_{span}]$.

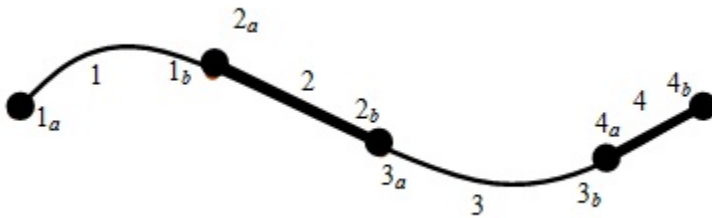


Figure 3. Direct element method: reference path decomposed in four elements

The angular acceleration \dot{r}_n , velocity r_n and position θ_n , in each element, are described then as follows:

$$\dot{r}_n = \int_0^{t_{nspan}} \ddot{r}_n \cdot dt = d_{3n} \cdot t_n + d_{2n} \quad (9)$$

$$r_n = \int_0^{t_{nspan}} \dot{r}_n \cdot dt = d_{3n} \cdot t_n^2 + d_{2n} \cdot t_n + d_{1n} \quad (10)$$

$$\theta_n = \int_0^{t_{nspan}} r_n \cdot dt = \frac{1}{6} \cdot d_{3n} \cdot t_n^3 + \frac{1}{2} \cdot d_{2n} \cdot t_n^2 + d_{1n} \cdot t_n + d_{0n} \quad (11)$$

Time span t_{nspan} is chosen either by decomposing the total manoeuvring time

$\sum_{n=1}^N t_{nspan} = T$ in N equal segments or by considering other parameters such as the change

of road curvature. The unknown states $y_n = [\dot{r}_{n,a} \quad r_{n,a} \quad \theta_{n,a} \quad \dot{r}_{n,b} \quad r_{n,b} \quad \theta_{n,b}]$ at the element's nodes are expressed in matrix form as:

$$y_n = A_n \cdot x_n$$

$$y_n = [\dot{r}_{n,a} \quad r_{n,a} \quad \theta_{n,a} \quad \dot{r}_{n,b} \quad r_{n,b} \quad \theta_{n,b}]^T \quad (12)$$

$$x_n = [d_{3n} \quad d_{2n} \quad d_{1n} \quad d_{0n}]^T$$

$$\mathbf{A}_n = \begin{bmatrix} 0 & 1 & 0 & 0 \\ 0 & 0 & 1 & 0 \\ 0 & 0 & 0 & 1 \\ t_{nspan} & 1 & 0 & 0 \\ 0.5 \cdot t_{nspan}^2 & t_{nspan} & 1 & 0 \\ 0.1667 \cdot t_{nspan}^3 & 0.5 \cdot t_{nspan}^2 & t_{nspan} & 1 \end{bmatrix}$$

Matrix \mathbf{A}_n constitutes the basis for joining the elements and deriving the system's solution \mathbf{y}_n , $n=1:N$. For more details on how many elements are needed, how to join them and how to introduce the boundary and intermediate conditions the reader is referred to [34].

An advantage of the direct element method is that a collision free path is obtained already from the first solution. Subsequently an optimization algorithm can be used to further optimize the path dynamics.

3. Vehicle slip prediction and path optimization

3.1 Vehicle slip prediction

The tire force F_y in the lateral direction is a nonlinear function of tire's slip angle α . However, for small slip angles a linear relation exists and therefore front F_{y1} and rear F_{y2} tire lateral forces can be expressed as $F_{yf} = C_f \cdot \alpha_f$ and $F_{yr} = C_r \cdot \alpha_r$, where C_f ,

α_f and C_r , α_r are the cornering stiffness and slip angle on the front and rear tire respectively. It is assumed that a tire cornering stiffness estimator like the one described in [40], [41] is utilized. In this case, Equations (1) & (2) are written also as:

$$m \cdot \dot{v} + \frac{1}{u_f} \cdot (C_f + C_r) \cdot v + \left\{ m \cdot u_f + \frac{1}{u_f} \cdot (l_f \cdot C_f - l_r \cdot C_r) \right\} \cdot r = C_f \cdot \delta \quad (13)$$

$$I \cdot \dot{r} + \frac{1}{u_f} \cdot (l_f^2 \cdot C_f + l_r^2 \cdot C_r) \cdot r + \frac{1}{u_f} \cdot (l_f \cdot C_f - l_r \cdot C_r) \cdot v = a \cdot C_f \cdot \delta \quad (14)$$

Under the hypothesis that velocity v is described, in each finite element, by a third order polynomial:

$$v = b_{3n} \cdot t^3 + b_{2n} \cdot t^2 + b_{1n} \cdot t + b_{0n} \quad (15)$$

then by substituting Equation (15) in Equations (13), (14) and combining them the following equation is obtained:

$$\begin{aligned}
& \left\{ \left[\frac{1}{u_f} \cdot (C_f + C_r) - \frac{1}{u_f \cdot l_f} \cdot (l_f \cdot C_f - l_r \cdot C_r) \right] \cdot t^3 + 3 \cdot m \cdot t^2 \right\} \cdot b_{3n} \\
& + \left\{ \left[\frac{1}{u_f} \cdot (C_f + C_r) - \frac{1}{u_f \cdot l_f} \cdot (l_f \cdot C_f - l_r \cdot C_r) \right] \cdot t^2 + 2 \cdot m \cdot t \right\} \cdot b_{2n} \\
& + \left\{ \left[\frac{1}{u_f} \cdot (C_f + C_r) - \frac{1}{u_f \cdot l_f} \cdot (l_f \cdot C_f - l_r \cdot C_r) \right] \cdot t + m \right\} \cdot b_{1n} \\
& + \left[\frac{1}{u_f} \cdot (C_f + C_r) - \frac{1}{u_f \cdot l_f} \cdot (l_f \cdot C_f - l_r \cdot C_r) \right] \cdot b_{0n} = I \cdot \dot{r} + \\
& \quad + \left\{ \frac{l_f^2 \cdot C_f + l_r^2 \cdot C_r}{u_f} - \left[l_f \cdot m \cdot u_f + \frac{l_f}{u_f} \cdot (l_f \cdot C_f - l_r \cdot C_r) \right] \right\} \cdot r
\end{aligned} \tag{16}$$

Equation (16) holds - at least - for one point (collocation point) in each element. Furthermore, if it is required for velocity v and its first two derivatives to be continuous over two consecutive elements:

$$v_{n,b} = v_{n+1,a} \tag{17}$$

$$\dot{v}_{n,b} = \dot{v}_{n+1,a} \tag{18}$$

$$\ddot{v}_{n,b} = \ddot{v}_{n+1,a} \tag{19}$$

three more equations are acquired. For N elements there are $N_u=4 \cdot N$ unknown coefficients and $N_c=N+(N-1) \cdot 3=4 \cdot N-3$ constraints. The rest three equations, so that $N_u=N_c$, are obtained from the following boundary conditions:

$$v_{1,a} = v(t = 0) \quad (20)$$

$$v_{N,b} = v(t = T) \quad (21)$$

$$\dot{v}_{N,b} = \dot{v}(t = T) \quad (22)$$

Four (4) elements are required to obtain a solution. The solution of the linear system of Equations (15)-(22), gives the coefficients $b_{3n}, b_{2n}, b_{1n}, b_{0n}$ for $n=1\dots N$ and thus the vehicle slip v and slip angle $\beta = \frac{v}{u_f}$ for the entire manoeuvre.

In the same line of thought, it is hypothesized that the steering input δ is described by a third order polynomial in each finite element:

$$\delta = c_{3n} \cdot t^3 + c_{2n} \cdot t^2 + c_{1n} \cdot t + c_{0n} \quad (23)$$

By combining Equations (14), (15) and (23) the coefficients c_{3n}, c_{2n}, c_{1n} and c_{0n} are expressed as:

$$c_{3n} = \frac{1}{u_f \cdot l_f \cdot Cf} \cdot (l_f \cdot Cf_1 - l_r \cdot Cr) \cdot b_{3n} \quad (24)$$

$$c_{2n} = \frac{1}{u_f \cdot l_f \cdot C_f} \cdot (l_f^2 \cdot C_f + l_r^2 \cdot C_r) \cdot \frac{1}{2} \cdot d_{3n} + \frac{1}{u_f \cdot l_f \cdot C_f} \cdot (l_f \cdot C_f - l_r \cdot C_r) \cdot b_{2n} \quad (25)$$

$$c_{1n} = \frac{1}{l_f \cdot C_f} \cdot I_z \cdot d_{3n} + \frac{1}{u_f \cdot l_f \cdot C_f} \cdot (l_f^2 \cdot C_f + l_r^2 \cdot C_r) \cdot d_{2n} + \frac{1}{u_f \cdot l_f \cdot C_f} \cdot (l_f \cdot C_f - l_r \cdot C_r) \cdot b_{1n} \quad (26)$$

$$c_{0n} = \frac{d_{2n}}{l_f \cdot C_f} + \frac{1}{u_f \cdot l_f \cdot C_f} \cdot (l_f^2 \cdot C_f + l_r^2 \cdot C_r) \cdot d_{1n} + \frac{1}{u_f \cdot l_f \cdot C_f} \cdot (l_f \cdot C_f - l_r \cdot C_r) \cdot b_{0n} \quad (27)$$

Obviously different path decomposition -selection of $t_{n\text{span}}$ - leads to different reference path. In general, there are infinite reference paths that satisfy the boundary conditions. The reason for using, usually in the first step, uniform path decomposition is because all elements share the same matrix \mathbf{A}_n and the linear system of equations can be solved with less computational burden.

3.2 Minimum vehicle slip v path planning

The reference path is computed for a manoeuvring period T which is usually determined by the time to collision (TTC) algorithm [32]. The initial partition t_{nspan}^0 of elements is chosen by uniformly decomposing the total manoeuvring time T in N segments or by considering other parameters such as the change of road curvature.

The partition chosen initially might not be optimal in terms of the vehicle slip angle β response. It is possible to repartition the manoeuvring time and get a reference path that causes lower slip angles β . Changing the initial partition is a computationally complex task because the problem is characterized by numerous local minima. Well-known optimization algorithms as the Nelder-Mead algorithm, Broyden-Fletcher-Goldfarb-Shanno algorithm and genetic algorithms have been tested and failed to find an optimal solution or weren't real time capable [42]. In this study we propose an empirical formula to calculate a new input $t_{nspan,cmd}^{i+1}$ for the elements' repartition. The main idea behind the

iterative algorithm is to reduce the maximum slip angle by equally distributing the “work” done $\int_0^{t_{nspan}} \beta \cdot dt$ in each element. For more details the reader is referred to [43]. In

particular the following formula is employed:

$$t_{nspan,cmd}^{i+1} = \frac{\left| \frac{b_{3n}}{4} \cdot t_{nspan}^4 + \frac{b_{2n}}{3} \cdot t_{nspan}^3 + \frac{b_{1n}}{2} \cdot t_{nspan}^2 + b_{0n} \cdot t_{nspan} \right|}{\sum_{n=1}^N \left(\left| \frac{b_{3n}}{4} \cdot t_{nspan}^4 + \frac{b_{2n}}{3} \cdot t_{nspan}^3 + \frac{b_{1n}}{2} \cdot t_{nspan}^2 + b_{0n} \cdot t_{nspan} \right| \right)} \cdot T \quad (28)$$

A first order stable iterative algorithm has been designed and uses $t_{nspan,cmd}^{i+1}$ as an input:

$$\frac{d(t_{nspan}^i)}{di} + \kappa \cdot t_{nspan}^i = t_{nspan,cmd}^{i+1} \quad (29)$$

$$\frac{t_{nspan}^{i+1} - t_{nspan}^i}{di} + \kappa \cdot t_{nspan}^i = t_{nspan,cmd}^{i+1} \quad (30)$$

$$t_{nspan}^{i+1} = (1 - \kappa \cdot di) \cdot t_{nspan}^i + di \cdot t_{nspan,cmd}^{i+1} \quad (31)$$

where i is the iteration number and κ a coefficient chosen by the user. It has been found that a selection $1 - \kappa \cdot di = 0.1$ works well in practice.

Obviously, the performance of the method depends on the accurate estimation of vehicle parameters used in Equations (16), (24)-(27). There are many techniques that can be employed prior to the initiation of a manoeuvre to improve the quality of estimation. Nevertheless, the method is flexible and computationally efficient so it can re-plan a path along a manoeuvre if a better estimation of vehicle parameters or target objects is available (e.g. moving obstacles). It is stressed that with the proposed method the transition from the old to the new path will be smooth.

4. Numerical examples – Discussion

In the following three numerical examples are presented and analysed. The results and their discussion show the proposed method's performance and its advantages over other known methods.

4.1 Case 1: Reference path on a straight line road segment: $Y_{des} = 3\text{ m}$ and

$$T = 2\text{ s}$$

In the first scenario, the host vehicle is approaching a stationary vehicle on a straight road segment. This represents a two-lane scenario with one lane blocked off. The goal is for the host vehicle to manoeuvre around the obstacle to the right using the available space including the hard shoulder.

The vehicle is moving at a speed $u_f = 80\text{ km/h}$. Suddenly, an obstacle at distance $d = 44.4\text{ m}$ appears in its direction of travel. The road surface is dry ($\mu = 1$). To avoid the collision the vehicle has to displace laterally by $Y_{des} = 3\text{ m}$. The vehicle parameters used in the first example are listed in Table 1.

Table 1 Vehicle & tire parameters used in case 1: VT1

Name	Parameter	Value
Vehicle mass	m [kg]	868
Distance from ground to CG	h [m]	0
Moment of inertia - to z axis	I_z [kg·m ²]	2877
Half length of the wheel axle	l [m]	0.765

Distance of front axle from cog	$l_f [m]$	1.3
Distance of rear axle from cog	$l_r [m]$	1.7
Front tire cornering stiffness	$C_f [N/rad]$	46000
Rear tire cornering stiffness	$C_r [N/rad]$	38000

A uniform element decomposition is chosen. The desired lateral displacement Y of the vehicle is shown in Figure 4a, while the computed steering input δ , Equations (23)-(27), in Figure 4b. The response of yaw rate r and lateral velocity v using the direct element method (de method) and their comparison with the numerical results obtained when integrating the vehicle Equations (int method), Eq. (1)-(2), are shown in Figure 5. For the integration the ode45 algorithm in Matlab was employed which is essentially an explicit Runge-Kutta 45 formula.

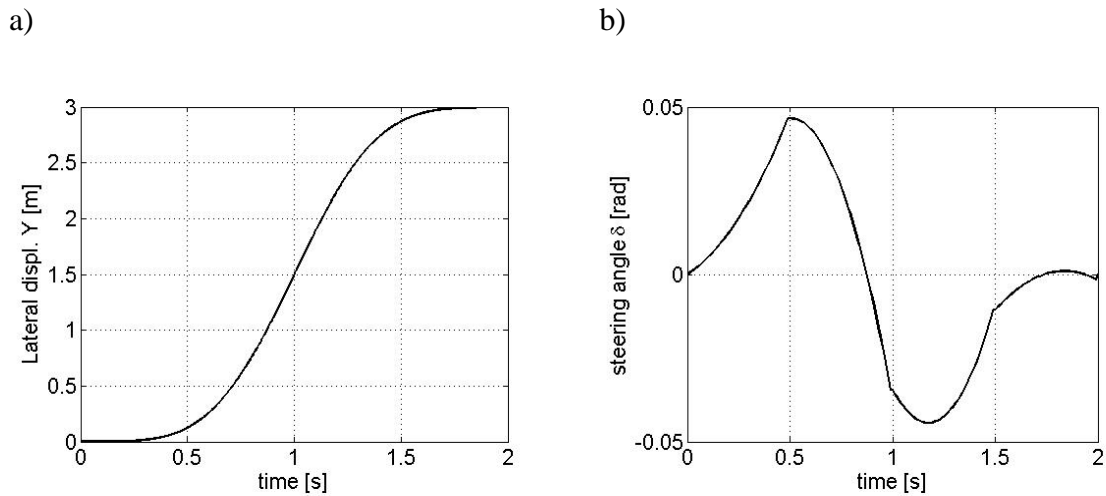
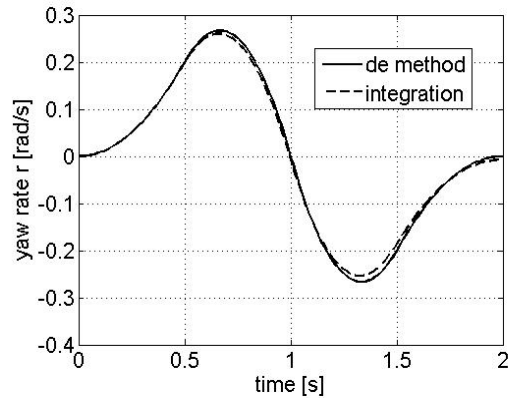


Figure 4. Case 1 – VT1: Reference path (left) and steering input (right)

a)



b)

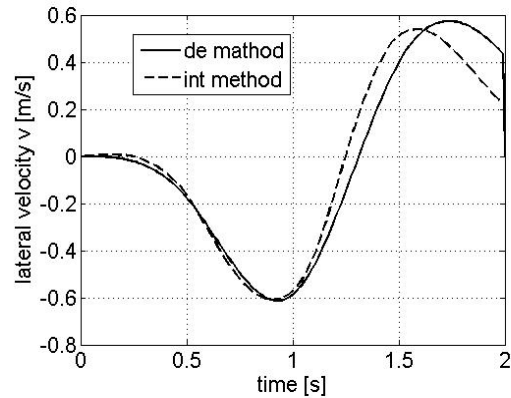


Figure 5. Case 1 – VT1: Yaw rate r (left) and lateral velocity v (right) response. Comparison between two methods

From the results it is observed that the steering input δ , computed by the direct element method, produces the desired reference path. The yaw rate response r between the direct element (de) and integration method is almost identical. The lateral velocity response v is quite similar but there is a phase difference, approximately 0.1 s, between them. The difference is because of the chosen collocation point. It has been validated, using an extensive number of trials, that a different collocation point may improve the phase error but will decrease the amplitude accuracy. There is a trade-off between phase and amplitude accuracy.

The performance of the method has been compared to other well known methods for a lane change manoeuvre presented in [9]. The case study is very similar to case study 1 with the only difference that the manoeuvring time is 2.5 s. The maximum lateral

acceleration and lateral jerk results of the proposed method, MPC, state lattice, cubic and quintic splines are listed and compared in Table 2.

Table 2 Maximum lateral acceleration and lateral jerk values for a case study described in [9] using the Direct Element, Model Predictive Control, State Lattice, Cubic Spline and Quintic Spline methods

	Results	
Method	Lateral acceleration [m/s^2]	Lateral jerk [m/s^3]
Direct Element	4.64	19
Model Predictive Control	5.1	20
State Lattice	4.7	14
Cubic Spline	6.1	14
Quintic Spline	6	18

The direct element method performs better compared to the other geometric path planning methods (cubic and quintic splines) and has a very similar response to the one obtained using MPC or state lattice. A further advantage of the direct element method compared to other geometric methods is the flexibility to include intermediate conditions. For example in Figure 6 the reference paths obtained for a varying intermediate condition $Y_{des}(t = 0.8 s) = [0.5, 0.75, 0.9] m$ are shown.

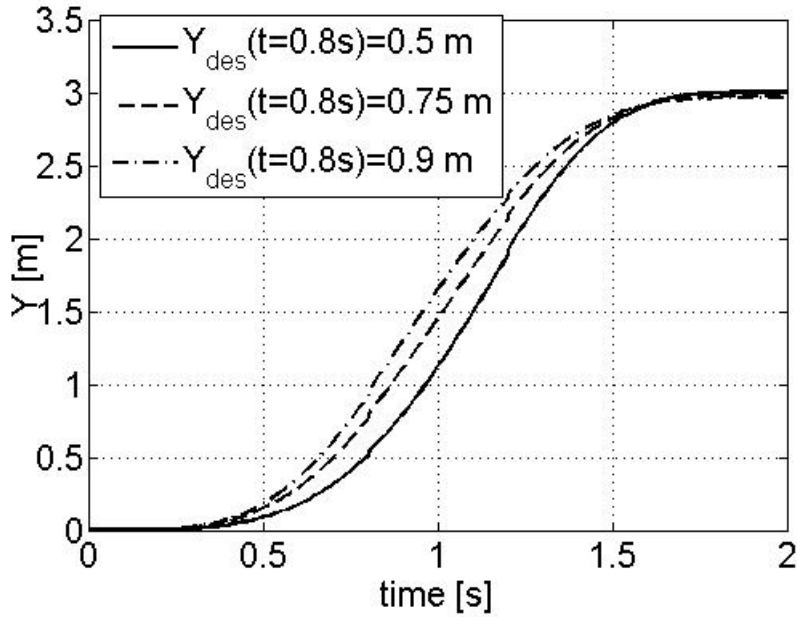


Figure 6. Case 1 – VT1: Reference paths under additional intermediate conditions

$$Y_{des}(t = 0.8 s) = [0.5, 0.75, 0.9] m$$

4.2 Case 2: Reference path generation with change in direction of travel:

$$Y_{des} = 3 m, \theta_{des} = 10^\circ \text{ and } T=2 s$$

In the second driving scenario the vehicle moves longitudinally on a road segment with a speed $u_f = 22.2 m/s$. The tire-road friction coefficient is $\mu = 1$. Due to road works, the vehicle has to displace laterally by $Y_{des} = 3 m$ and change its direction of travel by $\theta_{des} = 10^\circ$ within $T=2 s$. The proposed path planner is set to generate a reference path by using equally distanced elements.

The transient lateral displacement Y and respective steering input δ are plotted in Figures 7a & 7b. The comparison between yaw rate r and lateral velocity v results for the direct element and integration method are shown in Figures 8a & 8b. The vehicle parameters used in this example are listed in Table 3.

Table 3 Vehicle & tire parameters used in case 2: VT2

Name	Parameter	Value
Vehicle mass	m [kg]	1737
Distance from ground to CG	h [m]	0
Moment of inertia - to z axis	I_z [kgm ²]	2877
Half length of the wheel axle	l [m]	0.765
Distance of front axle from cog	l_f [m]	1.7
Distance of rear axle from cog	l_r [m]	1.3
Front tire cornering stiffness	C_f [N/rad]	46000
Rear tire cornering stiffness	C_r [N/rad]	56000

a)

b)

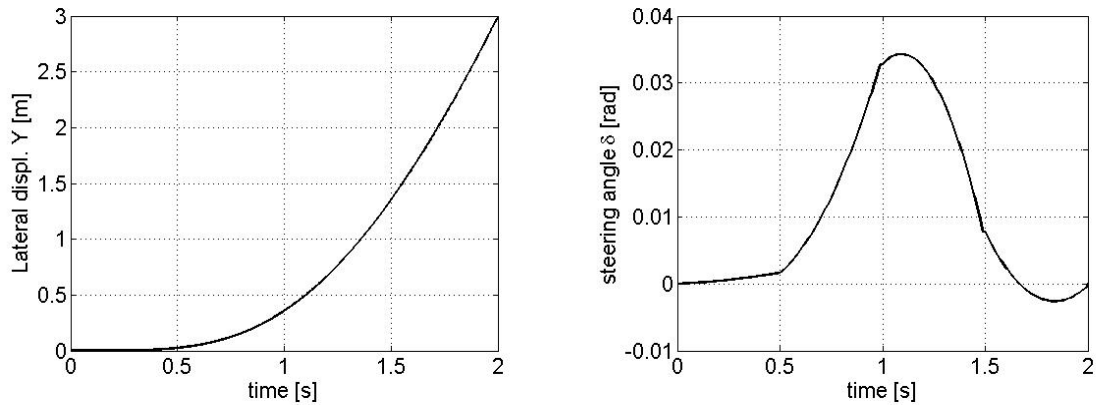


Figure 7. Case 2 – VT2: Reference path (left) and steering input (right)

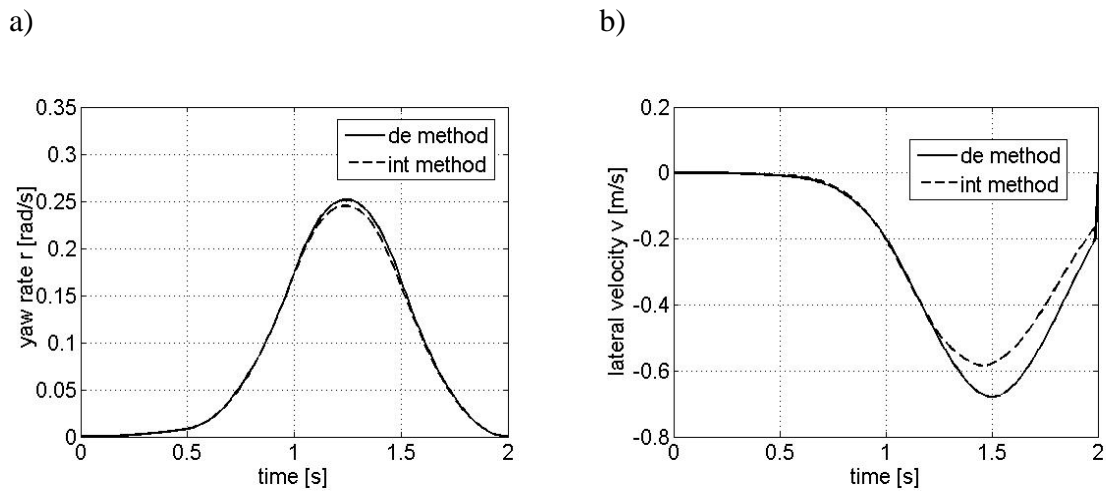


Figure 8. Case 2 – VT2: Yaw rate r (left) and lateral velocity v (right) response.

Comparison between two methods

Again, the calculated steering input produces the desired reference path. As in case 1, the yaw rate response r is almost identical between the two methods. Lateral velocity v is similar but there is an amplitude difference. With the direct element method a maximum

lateral velocity of 0.59 m/s is predicted, while with the integration one a maximum of 0.68 m/s . The error is approximately 15%.

The performance of the method has been compared to another one for a similar case study. In particular, a case was studied in which a vehicle driven at 19.44 m/s approaches a stationary target in a curve radius of 150 m . The manoeuvring time is $T=2.75 \text{ s}$. The test condition set up is severe as compared to highway/autobahn scenario where 150 m radius is rarely encountered [44]. The maximum yaw rate obtained using the direct element method and the one described in [44] are listed in Table 4. It is highlighted that the results using the direct element method were obtained for a uniform element partition.

Table 4 Maximum yaw rate values obtained in the case study described in [44] using the direct element method and the one in [44]

	Results
Method	Yaw rate [deg/s]
Direct Method	17.8
Shah et al (2013)	30

4.3 Case 3: Reference path optimisation: $Y_{des} = 3 \text{ m}$, $\theta_{des} = 10^\circ$, $r_{des} = 0.1 \text{ rad/s}$ and $T=1.5 \text{ s}$

The third driving scenario is utilized to derive an optimized reference path using the direct element method. It is hypothesized that the vehicle moves on a straight road segment with $u_f = 22.2 \text{ m/s}$ and that the friction coefficient is $\mu = 1$. The number of lanes

reduces from two to one at a distance $d = 33.3 \text{ m}$. The vehicle has to displace laterally by $Y_{des} = 3 \text{ m}$, change its direction of travel by $\theta_{des} = 10^\circ$ and enter a circular road segment with $r_{des} = 0.052 \text{ rad/s}$.

In the first iteration a reference path is planned using equally distanced elements. In the second iteration, a collision avoidance path is planned by redistributing the elements according to Equation (31). Table 5 lists the convergence of the iterative algorithm. As observed only a few iterations are required. If the computational cost is more important than accuracy then the result of the second iteration can already be utilized.

The transient lateral displacement Y for iterations 1, 2 and 3 are shown in Figure 9. The comparison between yaw rate r and lateral velocity v results (first and second iteration) are shown in Figures 10 and 11. The vehicle parameters VT2 are the same as in case 2. The dynamic properties of the two paths differ, as shown in Figures 9, 10 & 11. The maximum yaw rate r has reduced from 0.27 rad/s to 0.18 rad/s and the maximum lateral velocity v from 0.58 m/s to 0.44 m/s. The reduction in the maximum lateral velocity, and therefore the vehicle slip angle β , is approximately 25%.

Table 5 Case 3- VT2: Convergence of the iterative algorithm

	Iteration number			
	1	2	3	4
t_{n_span}				
Element 1	0.375 s	0.075 s	0.075 s	0.075 s
Element 2	0.375 s	0.465 s	0.3 s	0.285 s

Element 3	0.375 s	0.63 s	0.795 s	0.81 s
Element 4	0.375 s	0.33 s	0.33 s	0.33 s

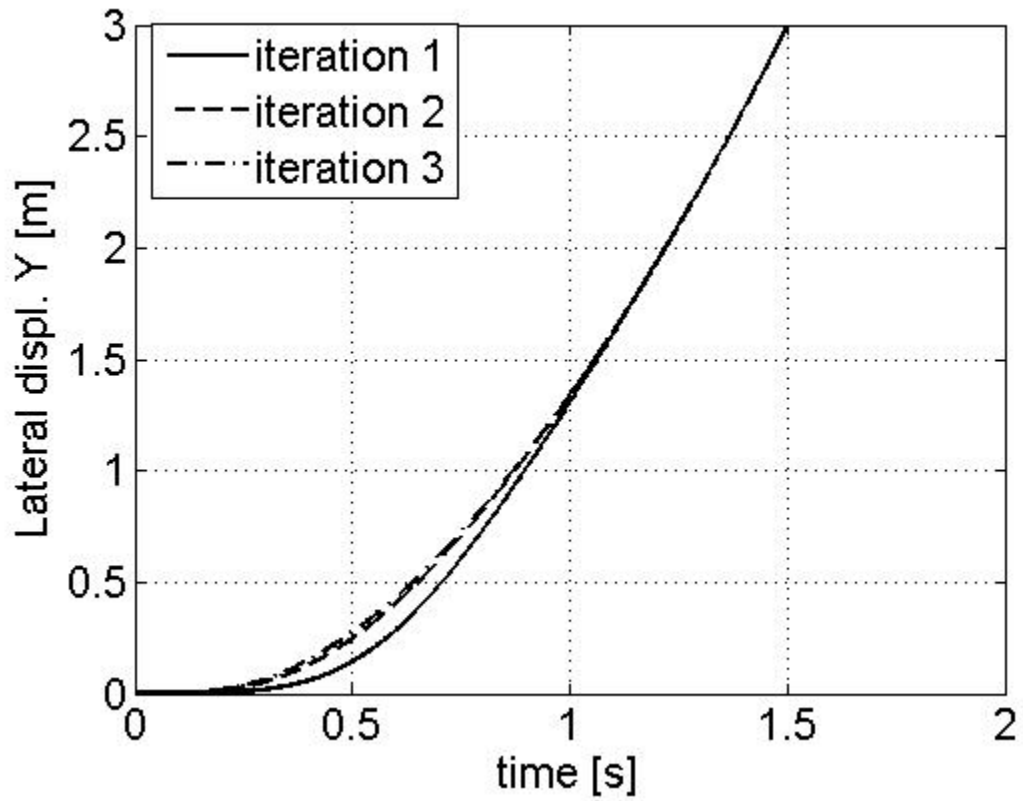


Figure 9. Case 3 – VT2: Convergence of reference paths

a)

b)

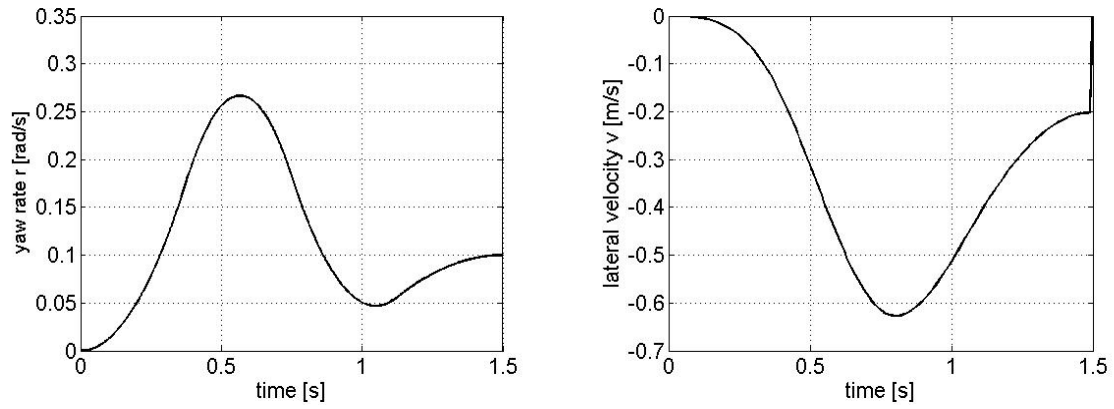


Figure 10. Case 3 – VT2: Yaw rate response r (left) and lateral velocity v (right) response using equally distributed elements

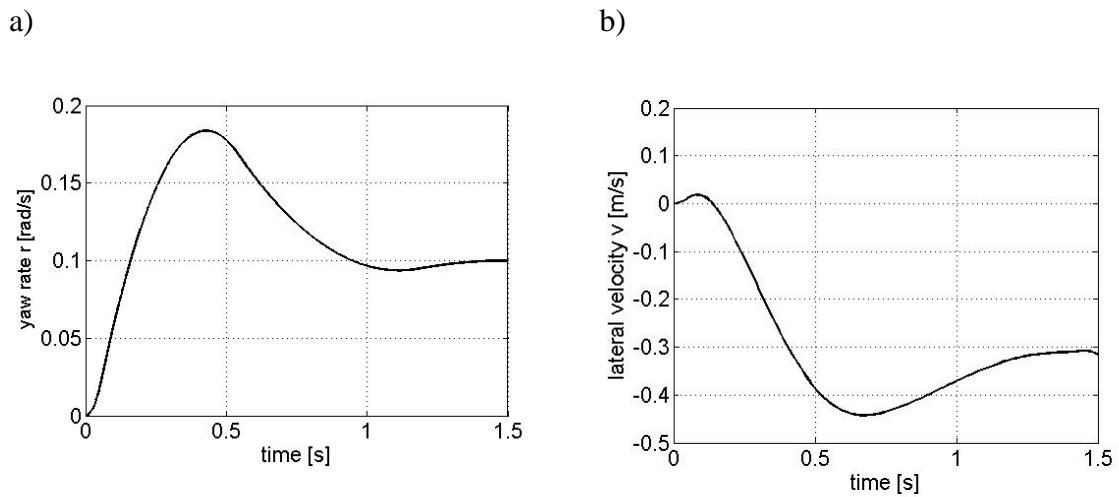


Figure 11. Case 3 – VT2: Yaw rate response r (left) and lateral velocity v (right) response using unequally distributed elements

5. Path optimization - Comparison between two vehicle configurations

In the direct element method, in the first step, a collision free path is calculated. The path primarily satisfies the desired boundary and intermediate conditions. It is usually obtained with a uniform element partition in which the vehicle configuration doesn't play any role. Vehicle slip is checked only against its limit, Equation (8).

On the other hand, in the second step the vehicle slip is utilized to plan an optimized path. The iterative algorithm in Equation (31) is used for this purpose. Different vehicle configurations exhibit different vehicle responses and therefore the resulting optimized reference paths are different.

For example, in the following, the optimized path in case 3 for another vehicle configuration is shown and discussed. The vehicle parameters are specified in Table 6 while the convergence of the iterative algorithm is given in Table 7. The optimized yaw rate and vehicle slip responses are illustrated in Figure 12.

The optimized element partition is different in the third configuration. The width of the second element is significantly reduced while those of elements 1 & 3 are reduced slightly. Furthermore, it is observed that although the vehicle yaw rate responses are quite the same the vehicle slip responses are quite different, refer to Figures 11 & 12. Although not shown here, it is mentioned that the optimized steering commands for the two vehicle configurations are completely different.

The vehicle parameter set VT3 used in this section is entirely different from the one VT2 used in the previous one. From numerous numerical experiments performed it has been concluded that a small variation of the vehicle parameters will not lead to a significant change of the elements optimized partition. Thus, the method is to a certain extent robust.

Table 6 Vehicle & tire parameters used in case 3: VT3

Name	Parameter	Value
Vehicle mass	m [kg]	868
Distance from ground to CG	h [m]	0
Moment of inertia - to z axis	I_z [kg·m ²]	1438
Half length of the wheel axle	l [m]	0.765
Distance of front axle from cog	l_f [m]	1.3
Distance of rear axle from cog	l_r [m]	1.7
Front tire cornering stiffness	C_f [N/rad]	38000
Rear tire cornering stiffness	C_r [N/rad]	46000

Table 7 Case 3 – VT3: Convergence of the iterative algorithm

	Iteration number			
	1	2	3	4
$t_{n\ span}$				
Element 1	0.375 s	0.05 s	0.05 s	0.05 s
Element 2	0.375 s	0.20 s	0.05 s	0.05 s
Element 3	0.375 s	0.7 s	0.72 s	0.72s
Element 4	0.375 s	0.05 s	0.18 s	0.18 s

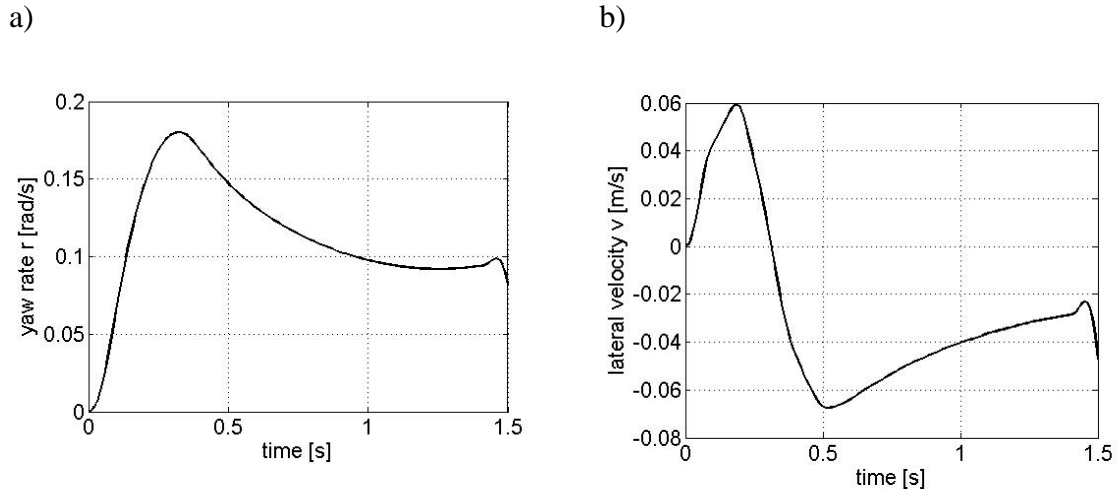


Figure 12. Case 3 – VT3: Yaw rate response r (left) and lateral velocity v (right) response using unequally distributed elements

6. Conclusions

Vehicle manufacturers and suppliers envision reducing fatalities and serious injuries to zero. However, in the UK the number of fatal accidents on rural roads is approximately double the one on urban and statistics showed that urban road accidents decreased less compared to other road types. Automated driving is proposed as a potential solution to this problem. Core in AD is the ability to plan safe and feasible paths that can match any road geometry and vehicle dynamics.

A literature survey has revealed that two categories of path planning methods mainly exist. One category uses iteratively forward vehicle model simulations while the second one uses mathematical functions to describe the geometry of the path (geometric path planning). In this study, a new method belonging to the second category is presented and discussed in detail.

One of the main contributions of this study is the development of a “geometric” method that predicts vehicle slip along the reference path. To our knowledge this is unique for a “geometric” path planning method. The second contribution is the development of an iterative algorithm that plans an optimized –with respect to vehicle slip- reference path.

The method has been evaluated for a number of case studies, typically found on rural road networks. A comparison with other methods, known from the literature, has shown its good performance because it performs better than most of the other methods. It has a small computational cost as it usually requires the solution of eight algebraic equations and a sparse 16×16 linear system. The method is very flexible since it is possible to define arbitrary boundary and any number of intermediate path conditions. The method usually converges within 2-3 iterations while with classical optimization algorithms it is very hard even to find the optimum solution. A further advantage is that the solution obtained in the first iteration is already a collision-free path.

In the future, a systematic study on the choice of the collocation point and its influence on the method’s performance need to be undertaken. Furthermore, the algorithm will be developed and tested for other case studies where time optimal solutions are sought e.g. minimum time cornering.

References

1. Assessment of Integrated Vehicle Safety Systems for improved vehicle safety.

See http://cordis.europa.eu/project/rcn/91187_en.html, Accessed 25/07/2015

2. Christensen, J.; Bastien, C.; Blundell, M.V.; Batt, P.A., Buckling considerations and cross-sectional geometry development for topology optimised body in white. *International Journal of Crashworthiness*. **2013** 18 (4), pp. 319-330
3. Bastien, C.; Neal-Sturgess, C.; Blundell, M.V. Influence of vehicle secondary impact following an emergency braking on an unbelted occupant's neck, head and thorax injuries. *International Journal of Crashworthiness*. **2013** 18 (3), pp. 215-224
4. Kanarachos, S. Design of an intelligent feed forward controller system for vehicle obstacle avoidance using neural networks. *International Journal of Vehicle Systems Modelling and Testing*. **2013** 8 (1), pp. 55-87
5. Stepper, K. New Safety Features for Crash Avoidance (2009) *Bosch*, See <http://www.casact.org/education/spring/2009/handouts/stepper.pdf>, Accessed 25/07/2015
6. Braun, P. Thrashing Swedish steel in the quest for a death-proof Volvo by 2020. See <http://www.digitaltrends.com/cars/volvo-xc90-zero-traffic-fatalities-injuries-2020/>, Accessed 25/07/2015
7. Rural Road Safety, The Royal Society for the Prevention of Accidents. [Available from <http://www.rosipa.com/road-safety/advice/road-users/rural>, Accessed 25/07/2015
8. Jeon, J.H.; Cowlagi, R.V.; Peters, S.C.; Karaman, S.; Frazzoli, E.; Tsiotras, P.; Iagnemma, K. Optimal motion planning with the half-car dynamical model for autonomous high-speed driving. In *Proceedings of the American Control Conference*. **2013** pp. 188-193

9. Madas, D.; Nosratinia, M.; Keshavarz, M.; Sundstrom, P.; Philippsen, R.; Eidehall, A.; Dahlen, K.-M. On path planning methods for automotive collision avoidance. In *Proceedings IEEE Intelligent Vehicles Symposium*, **2013**, pp. 931-937
10. Gray, A.; Gao, Y.; Lin, T.; Hedrick, J.K.; Tseng, H.E; Borrelli, F. Predictive control for agile semi-autonomous ground vehicles using motion primitives. In *Proceedings of the American Control Conference 2012*, **2012** 27–29 June 2012, pp. 4239–4244
11. Kuwata, Y.; Teo, J.; Fiore, G.; Karaman, S.; Frazzoli, E.; How, J.P. Real-time motion planning with applications to autonomous urban driving. In *IEEE Transactions on Control Systems Technology*, **2009**, *17* (5), pp. 1105-1118
12. Anderson, S.J.; Peters, S.C.; Pilutti, T.E.; Iagnemma, K. An optimal-control-based framework for trajectory planning, threat assessment, and semi-autonomous control of passenger vehicles in hazard avoidance Scenarios. *International Journal of Vehicle Autonomous Systems*, **2010**, *8* (2-4), pp. 190-216
13. Beal, C.E.; Gerdes, J.C. Model predictive control for vehicle stabilization at the limits of handling. In *IEEE Transactions on Control Systems Technology*. **2013**, *21* (4), art. no. 6226838, pp. 1258-1269
14. Son, Y.S.; Kim, W.; Lee, S.-H.; Chung, C. Robust Multi-rate Control Scheme with Predictive Virtual Lanes for Lane-keeping System of Autonomous Highway Driving. In *IEEE Transactions on Vehicular Technology*, **2014**, *99*, pp.1,1
15. Anderson, S.J.; Karumanchi, S.B.; Iagnemma, K. Constraint-based planning and control for safe, semi-autonomous operation of vehicles. In *Proceedings IEEE Intelligent Vehicles Symposium Proceedings*. **2012**, art. no. 6232153, pp. 383-388

16. Liu, J.; Jayakumar, P.; Stein, J.L.; Ersal, T. A multi-stage optimization formulation for MPC-based obstacle avoidance in autonomous vehicles using a LIDAR sensor. In *Proceedings ASME 2014 Dynamic Systems and Control Conference DSCC 2014*. **2014**, 2, no. 6269, pp. 1-10
17. Keviczky, T.; Falcone, P.; Borrelli, F.; Asgari, J.; Hrovat, D. Predictive control approach to autonomous vehicle steering. In *Proceedings of the American Control Conference 2006*. **2006**, pp. 4670-4675
18. Kim, D.; Kim, H. Lateral control for automated vehicle following system in urban environments. *SAE International Journal of Transportation Safety*. **2014** 2 (2), pp. 199-206
19. Lima P.; Trincavelli M.; Martensson J.; Wahlber B. Clothoid-Based Model Predictive Control for Autonomous Driving. *European Control Conference 15*. **2015**
20. Frasch, J.V.; Gray, A.; Zanon, M.; Ferreau, H.J.; Sager, S., Borrelli, F.; Diehl, M. An auto-generated nonlinear MPC algorithm for real-time obstacle avoidance of ground vehicles. In *Proceedings 2013 European Control Conference ECC 2013*. **2013**, pp. 4136-4141
21. Nilsson, J.; Falcone, P.; Ali, M.; Sjöberg, J. Receding horizon maneuver generation for automated highway driving. *Control Engineering Practice*. **2015**, 41, pp. 124-133
22. Hattori, Y., Ono, E., Hosoe, S. An optimum vehicle trajectory control for obstacle avoidance with the shortest longitudinal traveling distance. In *Proceedings of 2008 IEEE International Conference on Mechatronics and Automation ICMA 2008*. **2008** pp. 13-20

23. Kanarachos, S. A new min-max methodology for computing optimised obstacle avoidance steering manoeuvres of ground vehicles. *International Journal of Systems Science*. **2014** 45 (5), pp. 1042-1057
24. Tavernini, D.; Massaro, M.; Velenis, E.; Katzourakis, D.I.; Lot, R. Minimum time cornering: The effect of road surface and car transmission layout. *Vehicle System Dynamics*. **2013** 51 (10), pp. 1533-1547
25. Berntorp, K.; Olofsson, B.; Lundahl, K.; Nielsen, L. Models and methodology for optimal trajectory generation in safety-critical road-vehicle manoeuvres. *Vehicle System Dynamics*. **2014** 52 (10), pp. 1304-1332
26. Chakraborty, I., Tsiotras, P., Diaz, R.S. Time-optimal vehicle posture control to mitigate unavoidable collisions using conventional control inputs. In *Proceedings of the American Control Conference*. **2013**, pp. 2165-2170
27. Snider, J. M. Automatic Steering Methods for Autonomous Automobile Path Tracking. tech. report CMU-RI-TR-09-08, Robotics Institute, *Carnegie Mellon University*. **2009**
28. Gray, A.; Gao, Y.; Lin, T.; Hedrick, J.K.; Tseng, H.E.; Borrelli, F. Predictive control for agile semi-autonomous ground vehicles using motion primitives. In *Proceedings of the American Control Conference*. **2012**, pp. 4239-4244
29. Dai, P.; Katupitiya, J. Path planning and tracking of a 4WD4WS vehicle to be driven under force control, In *Proceedings 2014 IEEE International Conference on Mechatronics and Automation IEEE ICMA 2014*. **2014**, pp. 1709-1715

30. Funke, J.; Gerdes, J.C. Simple clothoid paths for autonomous vehicle lane changes at the limits of handling. In *Proceedings ASME 2013 Dynamic Systems and Control Conference DSCC 2013*. **2013** 3, art. no. V003T47A003
31. Shim, T.; Adireddy, G.; Yuan, H. Autonomous vehicle collision avoidance system using path planning and model-predictive-control-based active front steering and wheel torque control. *Proceedings of the Institution of Mechanical Engineers, Part D: Journal of Automobile Engineering*. **2012** 226 (6), pp. 767-778
32. Keller, C.G.; Dang, T.; Fritz, H.; Joos, A.; Rabe, C.; Gavrila, D.M. Active pedestrian safety by automatic braking and evasive steering. *IEEE Transactions on Intelligent Transportation Systems*, **2011** 12 (4), pp. 1292-1304
33. Isermann, R.; Mannale, R.; Schmitt, K. Collision-avoidance systems PRORETA: Situation analysis and intervention control. *Control Engineering Practice*. **2012** 20 (11), pp. 1236-1246
34. Kanarachos, S.; Alirezai, M. An adaptive finite element method for computing emergency manoeuvres of ground vehicles in complex driving scenarios. *International Journal of Vehicle Systems Modelling and Testing*. **2015** 10 (3), pp. 239-262
35. Berntorp, K.; Olofsson, B.; Bernhardsson, B.; Lundahl, K.; Nielsen, L. Models and methodology for optimal vehicle maneuvers applied to a hairpin turn. In *Proceedings of the American Control Conference*. **2013**, pp. 2139-2146
36. Lundahl, K.; Berntorp, K.; Olofsson, B.; Åslund, J.; Nielsen, L., Studying the Influence of Roll and Pitch Dynamics in Optimal Road-Vehicle Maneuvers. In

Proceedings of the 23rd International Symposium on Dynamics of Vehicles on Roads and Tracks. 2013 :

37. Pacejka, B., Tire and Vehicle Dynamics: Chapter 1. *Society of Automotive Engineers Warrendale.2005*
38. Rajamani, R. Vehicle Dynamics and Control: Chapters 2, 3 and 8. *Springer. 2012*
39. Alirezaei, M.; Kanarachos, S.; Scheepers, B.; Maurice, J.P., Experimental evaluation of optimal Vehicle Dynamic Control based on the State Dependent Ricatti Equation technique. In: *Proceedings of the American Control Conference. 2013*, pp. 408-412
40. Baffet, G.; Charara, A; Lechner, D. Estimation of vehicle sideslip, tire force and wheel cornering stiffness. *Control Engineering Practice. 2009 17 (11)*, pp. 1255–1264
41. Hewson, P., Method for estimating tyre cornering stiffness from basic tyre information. *Proc. IMechE Part D: J. Automobile Engineering. 2005 219*. pp. 1407-1412
42. Papalambros, P.; Wilde, D., Principles of optimal design: Modelling and computation. *Cambridge University Press, 2000*
43. Kanarachos, S., A new method for computing optimal obstacle maneuvers of vehicles. *International Journal of Vehicle Autonomous Systems. 2009 7(1)*, pp.73-95
44. Shah, J.; Benmimoun, A. Braking and Steering Interventions for Collision Avoidance. In *Proceedings 22nd Aachen Colloquium Automobile and Engine Technology. 2013*, pp. 739-750